



Contents lists available at ScienceDirect

Radiation Measurements

journal homepage: www.elsevier.com/locate/radmeas

Radiation dose in 320-detector-row CT coronary angiography: Prospective ECG triggering combined with multi-segment reconstruction

Ching-Ching Yang^a, Jay Wu^b, Chia-Jung Tsai^d, Chien-Chuan Chen^{c,d}, Chien-Fu Hung^{c,**,1}, Tung-Hsin Wu^{d,*}

^a Department of Radiological Technology, Tzu Chi College of Technology, Hualien, Taiwan

^b Department of Biomedical Imaging and Radiological Science, China Medical University, Taiwan

^c Department of Medical Imaging and Intervention, Chang Gung Memorial Hospital at Linkou, 5 Fushing 1st Rd., Taoyuan 333, Taiwan

^d Department of Biomedical Imaging and Radiological Sciences, National Yang-Ming University, 155 Li-Nong St., Sec. 2, Taipei 112, Taiwan

ARTICLE INFO

Article history:

Received 24 November 2010

Received in revised form

29 June 2011

Accepted 2 July 2011

Keywords:

320-Detector-row coronary CT angiography

Radiation dose

ECG pulsing window width

Heart rate

ABSTRACT

Background: The aim of this study was to investigate patient doses in prospective electrocardiogram (ECG)-triggered CT coronary angiography (CTCA) combined with multi-segment reconstruction on a 320-detector-row CT.

Methods: CTCA data acquired with prospective ECG (pECG) triggering at 0–100% (pECG_{100%}), 30–80% (pECG_{50%}), 70–80% (pECG_{10%}) of the R–R interval and reconstructed using mono-, two- and three-segment reconstruction were investigated. Effective doses were estimated by using LiF-TLDs placed at several organ sites in an Alderson-Rando phantom.

Results: With pECG_{100%}, the estimation of effective dose of data reconstructed using mono-segment (pECG_{100%_1S}) reconstruction was 10.01 ± 0.56 mSv. For data acquired using pECG_{50%}, the effective doses were 6.16 ± 0.12 , 9.92 ± 0.37 and 13.51 ± 0.17 mSv in mono-segment (pECG_{50%_1S}), two-segment (pECG_{50%_2S}) and three-segment (pECG_{50%_3S}) reconstruction, respectively. The effective dose of data acquired with pECG_{10%} and reconstructed using mono-segment (pECG_{10%_1S}) reconstruction was 3.61 ± 0.07 mSv. We observed a difference of around 7.46% between effective doses estimated using TLD-phantom measurement and CT dose index (CTDI) obtained from the scanner.

Conclusion: For patients with low and intermediate heart rate, radiation exposure could be reduced by 38.6% or more by narrowing pulsing window width. Although slightly higher radiation dose was observed in multi-segment reconstruction, this method can be used in high heart rate patients to provide data of high temporal resolution without increasing radiation exposure when it is combined with prospective ECG triggering.

© 2011 Elsevier Ltd. All rights reserved.

1. Introduction

The 320-detector-row CT system is comprised of 320×0.5 mm detector rows and a gantry rotation time of 350 ms. The increased anatomical coverage and gantry rotation time allow image acquisition of the entire heart within a single heartbeat for patient with heart rate (HR) <65 beats per minute (bpm). The entire dataset is temporally uniform, so its image quality is less affected by cardiac and respiratory motion artifacts. In addition, because extra or overlapping rotation is no longer necessary in 320-detector-row CT

examinations, patient exposure could be decreased markedly (Pasricha et al., 2009; Dewey et al., 2009; de Graaf et al., 2010; van der Bijl et al., 2010). In patients with HR > 65 bpm, the multi-segment reconstruction algorithm is recommended to improve temporal resolution. But this leads to increased radiation exposure because data are acquired during two or more consecutive heartbeats (Leschka et al., 2008; Herzog et al., 2007). Prospective electrocardiogram (ECG)-triggering acquisition has been proven to be an important strategy for radiation dose reduction in CT coronary angiography (CTCA). A study of radiation dose of a dual-source 64-slice CT reported that a mean effective dose of 7.6 mSv from retrospective ECG gating can be reduced to 3.4 mSv when using prospective ECG gating (Hein et al., 2009). The aim of this study was to investigate the reduction of radiation dose on a 320-detector-row CT coronary angiography using ECG-triggered scan combined with multi-segment reconstruction techniques.

* Corresponding author. Tel.: +886 2 28267061.

** Corresponding author. Tel.: +886 3 3281200x2575.

E-mail addresses: hcf5514@adm.cgmh.org.tw (C.-F. Hung), tung@ym.edu.tw (T.-H. Wu).

¹ C.F. Hung and T.H. Wu contributed equally to this work.

For CT dose evaluation, the conventional CT dose index (CTDI) is no longer applicable in CT scanners with a detector length >10 cm (Huda et al., 2010; Elojeimy et al., 2010; Mori et al., 2005; Geleijns et al., 2009; Lin and Herrnsdorf, 2010; Diekmann et al., 2010). The CTDI methodology of dosimetry in wide area detector CT has been studied by many investigators. Geleijns et al. (2009) investigated various dosimetric CTDI metrics with extended pencil CT ionization chamber (300, 600 mm) in combination with extended CT dosimetry phantoms (350, 700 mm). They suggested that CTDI_{300 w} measured in 350 mm long CT dosimetry phantom is an appropriate dose quantity for the 320-detector-row CT. They also concluded that difference between radiation doses obtained using conventional and extended approaches can be corrected using the dose ratio between the two dosimetry methods. Lin and Herrnsdorf (2010) proposed a pseudohelical scan in order to determine a reasonable setup of CT dosimetry phantom and ionization chamber. In this work, they recommended that the CT dosimetry phantom needs to be at least 750 mm long to measure the radiation dose profile for CT scanner with a beam width of 160 mm. To overcome controversy between different CTDI definitions, we primarily used TLD-phantom measurement in this study to achieve accurate and reproducible results for 320-detector-row CTCA.

2. Materials and methods

2.1. TLD-based in-phantom dosimetry

An anthropomorphic phantom (Rando Alderson phantom; Radiology Support Devices, Long Beach, CA) simulating the body of a 170 cm tall, 70 kg man and LiF-TLD (TLD-100H; Bicron–Harshaw, Solon, OH, USA) were used in this study. The phantom consisted of 35 sections with thickness of 2.5 cm is composed of a natural human skeleton embedded in a mass with the properties of human soft tissue (mass density, $\rho = 0.985 \text{ kg/dm}^3$; effective atomic number, $Z_{\text{eff}} = 7.3$), and its thorax is made of foam ($\rho = 0.32 \text{ kg/dm}^3$; $Z_{\text{eff}} = 7.3$) to simulate human lung tissue. A total of 76 TLDs were placed within the anthropomorphic phantom to estimate radiation dose of brain (4 TLDs), thyroid (4 TLDs), esophagus (4 TLDs), lungs (4 TLDs), stomach (4 TLDs), liver (4 TLDs), bladder (4 TLDs), colon (4 TLDs), testicles (4 TLDs), heart (4 TLDs), kidneys (4 TLDs), small intestine (4 TLDs), skin (12 TLDs) and red bone marrow (16 TLDs) (Wu et al., 2004). According to International Commission on Radiological Protection (ICRP) 103 (2007), heart, kidneys and small intestine were categorized into the remainder tissue. The skin dose was measured by using TLDs attached in eyes, thorax and abdominal surface. Skin values measured at the thoracic region were used to estimate the doses received by breast. Radiation dose to red bone marrow was measured in ribs, thoracic spinal column, lumbar spinal column and pelvis. We calibrated the TLDs according to the tube potential: 120 kV, 6.58 mm Al filtering. The TLDs were read out after heating and annealing (TLD oven; Furnaces-Muffle, Type 47900, Thermolyne) in a TLD reader (UL-320, TLD Systems & Components, Inc.) within 24 h of measurement. Using the TLD batch calibration factor, absorbed doses were determined at each TLD location. The mean absorbed doses were then calculated from the TLDs distributed throughout each organ. Next, the absorbed doses for each organ were converted into tissue-weighted equivalent doses using the ICRP 103 tissue weighting factors:

$$H_E = \sum D_T \cdot w_R \cdot w_T \quad (1)$$

where D_T is the mean dose to the target organ, w_R is the radiation weighting factor (for X-ray, $w_R = 1$), and w_T is the tissue weighting factor. Finally, these tissue-weighted equivalent doses were summed to yield the total effective dose.

2.2. CT data acquisition and reconstruction

CT examinations were performed on a 320-detector-row CT scanner (Aquilion ONE, Toshiba Medical Systems, Otawara, Japan) with 350 ms of gantry rotation time (T_{rot}) using prospective ECG triggering. The ECG-triggered scan can be adapted according to the HR for radiation dose reduction while maintaining diagnostic image quality. Commonly, full tube current is used between 30% and 80% of the R–R interval to acquire data from end-systolic to end-diastolic phase. In patient with low and stable HR (<65 bpm), radiation dose can be further reduced by using ECG pulsing window at 70–80% of the R–R interval to acquire data at late diastole. Fig. 1 shows a schematic view of prospective ECG (pECG) triggering at 0–100% (pECG_{100%}), 30–80% (pECG_{50%}) and 70–80% (pECG_{10%}) of the R–R interval. In patients with HR ≤ 65 bpm, scanning was completed within a single heartbeat using a 180° segment, thus providing an effective temporal resolution of 175 ms ($T_{\text{rot}}/2$). A switch to multi-segment acquisition was automatically triggered by the system when HR > 65 bpm. In patients with HR between 65 bpm and 80 bpm, 2 heartbeats were used for image acquisition to generate image with temporal resolution in the interval $[T_{\text{rot}}/4, T_{\text{rot}}/2]$. Datasets for patients with HR > 80 bpm were acquired during 3 heartbeats. The images reconstructed using three-segment-method have temporal resolution in the interval $[T_{\text{rot}}/6, T_{\text{rot}}/2]$. Fig. 2(a)–(c) show a schematic view of data acquired using pECG_{50%} and reconstructed with mono-segment (pECG_{50%_1S}), two-segment (pECG_{50%_2S}) and three-segment (pECG_{50%_3S}) reconstruction for HR = 60, 75 and 85 bpm, respectively. To investigate the impact of ECG pulsing and reconstruction mode on patient radiation dose, patient cardiac simulator (Cardiac Trigger, Model: CTM300, IVY biological system, Inc.) was used to simulate

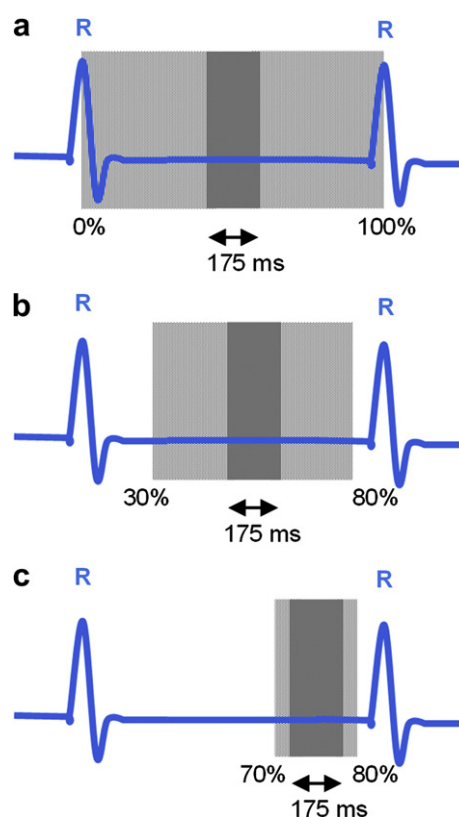


Fig. 1. CT examination performed using pECG_{100%} (a), pECG_{50%} (b) and pECG_{10%} (c). The dark gray areas represent the minimum acquisition window for half scan reconstruction. The light gray areas represent padding duration.

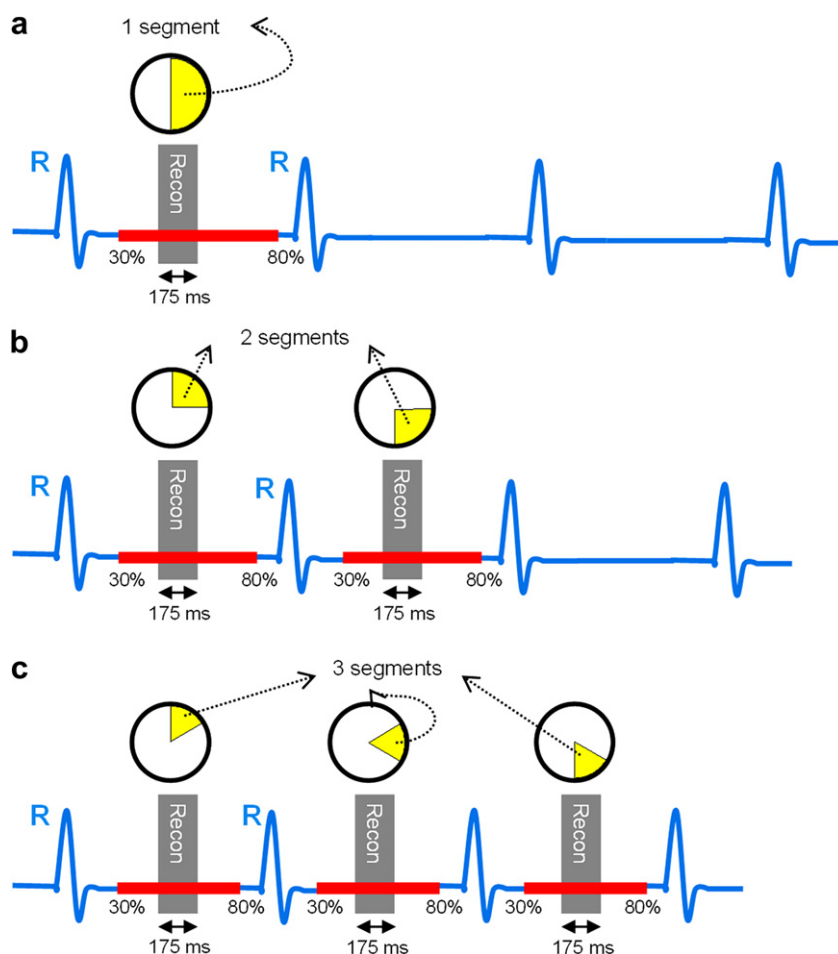


Fig. 2. (a) Mono-, (b) two- and (c) three-segment reconstructions for data acquired using pECG_{50%}. The thicker lines represent ECG pulsing window. One half gantry rotation data were used for image reconstruction (gray rectangles).

patients with mean HR of 60, 75 and 85 bpm. Table 1 lists five pECG scan protocols examined in this study. Besides the protocols shown in Fig. 2, we also included scan protocols performed using pECG_{100%} and reconstructed with mono-segment reconstruction (pECG_{100%_1S}) and performed using pECG_{10%} and reconstructed with mono-segment reconstruction (pECG_{10%_1S}). CT scanning was performed with no table movement (pitch = 0), 0.5 mm detector elements, 400 mA tube current and 120 kV tube voltage. Data were reconstructed at 0.5-mm slice thickness with 0.25-mm intervals.

3. Results

Although the largest available nominal beam width is 160 mm for the scanner, a 128 mm axial coverage is sufficient to cover the heart volume for most patients. Based on our results, effective dose

obtained from 160 mm axial coverage is about 1.32–1.51 times higher than that obtained from 128 mm axial coverage (data not shown). Therefore, in the present study we restricted z-axis coverage to a 128-mm field-of-view. Table 2 summarizes the result of mean absorbed dose in various organs estimated from the TLD-phantom measurement. Using the TLD results and ICRP 103 tissue-weighted factors, effective doses for five pECG scan protocols were calculated. They were 10.03 ± 0.56 , 6.17 ± 0.14 , 3.62 ± 0.12 , 9.40 ± 0.37 and 13.54 ± 0.28 mSv for pECG_{100%_1S}, pECG_{50%_1S}, pECG_{10%_1S}, pECG_{50%_2S}, and pECG_{50%_3S}, respectively. Fig. 3 shows the comparison of effective doses obtained from TLD-phantom measurement and CTDI method obtained from the scanner-output dose report. We observed a difference of around 7.46% between effective doses estimated from TLD-phantom measurement and CTDI method.

Table 1
Prospectively ECG-triggered (pECG) scan protocols.

	Mono-segment reconstruction			Multi-segment reconstruction	
	pECG _{100%_1S}	pECG _{50%_1S}	pECG _{10%_1S}	pECG _{50%_2S}	pECG _{50%_3S}
Tube voltage (kV)	120	120	120	120	120
Tube current (mA)	400	400	400	400	400
Heart rate (bpm)	<65	<65	<65	65–80	>80
Pulsing window	0–100%	30–80%	70–80%	30–80%	30–80%
Reconstruction mode	Mono-segment	Mono-segment	Mono-segment	Two-segment	Three-segment

Table 2
Mean absorbed doses in various organs estimated using TLD-phantom measurement.

Organ	Tissue Weighting Factor	Mean Absorbed Dose (mGy)				
		pECG _{100%_1S}	pECG _{50%_1S}	pECG _{10%_1S}	pECG _{50%_2S}	pECG _{50%_3S}
Brain	0.01	0.12 ± 0.02	0.06 ± 0.01	0.04 ± 0.01	0.10 ± 0.01	0.27 ± 0.01
Thyroid	0.04	1.95 ± 1.37	1.43 ± 1.20	0.65 ± 0.49	1.68 ± 1.17	4.00 ± 0.69
Esophagus	0.04	7.01 ± 5.01	4.24 ± 2.44	2.54 ± 1.44	6.08 ± 3.96	12.26 ± 3.59
Lung	0.12	24.27 ± 1.44	12.31 ± 1.44	7.23 ± 1.35	22.34 ± 6.75	33.69 ± 4.59
Liver	0.04	7.82 ± 3.44	4.34 ± 1.97	2.74 ± 1.09	7.61 ± 1.70	10.32 ± 0.51
Stomach	0.12	6.80 ± 2.13	4.16 ± 0.89	3.15 ± 1.05	5.54 ± 0.34	7.60 ± 0.87
Colon	0.12	0.36 ± 0.10	0.19 ± 0.07	0.13 ± 0.08	0.29 ± 0.09	0.78 ± 0.04
Bladder	0.04	0.23 ± 0.06	0.13 ± 0.02	0.07 ± 0.03	0.22 ± 0.03	0.74 ± 0.04
Gonads	0.08	0.08 ± 0.01	0.05 ± 0.01	0.03 ± 0.02	0.08 ± 0.03	0.87 ± 0.01
Breast	0.12	22.06 ± 11.24	19.53 ± 4.47	10.95 ± 2.38	27.71 ± 12.63	33.32 ± 5.22
Bone marrow	0.12	19.85 ± 11.44	8.67 ± 4.99	4.89 ± 2.81	16.81 ± 9.68	21.83 ± 12.48
Skin	0.01	20.25 ± 12.14	17.92 ± 10.74	9.58 ± 5.83	25.53 ± 15.28	28.09 ± 17.12
Heart	0.00923	32.58 ± 5.80	18.37 ± 3.08	10.40 ± 1.43	31.65 ± 1.45	38.94 ± 1.50
Small intestines	0.00923	2.95 ± 1.12	1.99 ± 0.82	1.64 ± 0.78	2.86 ± 0.77	4.34 ± 0.77
Kidney	0.00923	2.09 ± 1.10	1.31 ± 0.88	1.13 ± 0.96	1.63 ± 0.84	3.54 ± 0.05
Total dose (dose ratio)	–	148.42	94.70 (1.62 ^a)	55.17 (2.77 ^a)	150.13 (1.61 ^b)	200.59 (2.19 ^b)

^a Ratio = dose from pECG_{100%_1S}/dose from the current protocol.

^b Ratio = dose from the current protocol/dose from pECG_{50%_1S}.

4. Discussion

For ECG triggering at 0–100%, 30–80% and 70–80% of the R–R interval, the X-ray exposure time for patients with HR = 60 bpm was around 1000, 675 and 275 ms, respectively. Therefore, a reasonable estimate of effective dose from pECG_{100%_1S} is around 1.48 times compared to that obtained from pECG_{50%_1S}. Similarly, the dose ratio between pECG_{100%_1S} and pECG_{10%_1S} should be around 3.63. The corresponding results from TLD-phantom measurement were 1.62 and 2.77. These results show that the use of ECG pulsing can decrease radiation dose by 38.6% or more. The slight discrepancy between estimated and calculated dose ratio may be due to the time required to ramp up and down the tube current. The X-ray generated within this duration is not for imaging, but would increase the patient exposure.

For TLD-phantom measurement, the ratio of radiation doses obtained using pECG_{50%_1S} and pECG_{50%_2S} was 1.61, and the ratio between pECG_{50%_1S} and pECG_{50%_3S} was 2.19. For segmented reconstruction, a complete half scan dataset was formed using sub-segments from consecutive heart cycles (Fig. 2(b) and (c)). Hence, a two-fold and three-fold increase in effective dose might be expected in two- and three-segment reconstructions, respectively, when compared with that in mono-segment reconstruction.

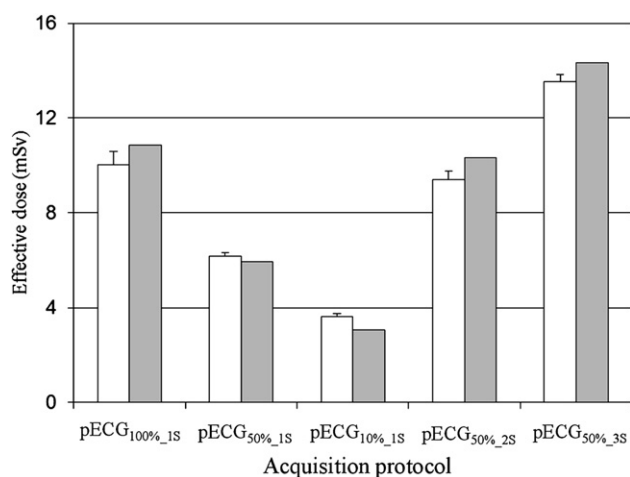


Fig. 3. Comparison between effective dose estimates obtained using TLD-phantom measurement (white columns) and CTDI-based method (gray columns).

However, for patients with higher HR, the X-ray beam-on time to cover the same cardiac phases is reduced (Fig. 2). For instance, the exposure time of ECG pulsing window at 30–80% of the R–R interval was around 675, 575 and 528 ms for patients with HR = 60, 75 and 85 bpm, respectively. Hence, a reasonable estimate of effective dose from pECG_{50%_2S} is around 1.70 times compared to that obtained from pECG_{50%_1S}. Similarly, the dose ratio between pECG_{50%_3S} and pECG_{50%_1S} should be around 2.35. Although radiation dose in multi-segment reconstruction is slightly higher than that in mono-segment reconstruction, it can be used in high HR patients to provide data of high temporal resolution without increasing radiation exposure when it is combined with prospective ECG triggering.

Several factors could cause error in our experimental results. First, according to previous studies, the integration range needs to be long enough to accurately measure doses from CT scanner with wide detector coverage due to scattered radiation (Mori et al., 2005; Geleijns et al., 2009; Lin and Herrnsdorf, 2010). The TLDs in the Rando phantom integrate exposure not only from primary radiation but also from high-intensity scattered radiation, which should produce more accurate estimates in CTCA. The locations of TLDs in Rando phantom may also introduce bias into the results. Hence, 4 or more TLDs were placed in each organ to lower the possible measurement uncertainty. Our results indicate that there is no relevant difference between the effective doses estimated using TLD-phantom measurement and CTDI method. This finding suggested that our study is technically adequate of the 320-detector CT scanner.

In conclusion, we have examined the impacts of HR-dependent ECG pulsing width and reconstruction mode on patient radiation dose using TLD-phantom measurement. For patients with low and intermediate HR (HR < 65 bpm), radiation exposure could be reduced by 38.6% or more by narrowing pulsing window width. Although slightly higher radiation dose was observed in multi-segment reconstruction, it can provide data of high temporal resolution without increasing radiation exposure for patients with high HR (HR > 65 bpm) when combined with prospective ECG triggering.

Acknowledgments

This study was financially supported by the National Science Council of Taiwan (NSC99-2314-B-010-043-MY3).

References

- de Graaf, F.R., Schuijf, J.D., van Velzen, J.E., et al., 2010. Diagnostic accuracy of 320-row multidetector computed tomography coronary angiography in the non-invasive evaluation of significant coronary artery disease. *Eur. Heart J.* 31, 1908–1915.
- Dewey, M., Zimmermann, E., Deissenrieder, F., et al., 2009. Noninvasive coronary angiography by 320-row computed tomography with lower radiation exposure and maintained diagnostic accuracy: comparison of results with cardiac catheterization in a head-to-head pilot investigation. *Circulation* 120, 867–875.
- Diekmann, S., Siebert, E., Juran, R., et al., 2010. Dose exposure of patients undergoing comprehensive stroke imaging by multidetector-row CT: comparison of 320-detector row and 64-detector row CT scanners. *AJNR Am. J. Neuroradiol.* 31, 1003–1009.
- Elojeimy, S., Tipnis, S., Huda, W., 2010. Relationship between radiographic techniques (kilovoltage and milliamperes-second) and CTDI(VOL). *Radiat. Prot. Dosim.* 141, 43–49.
- Geleijns, J., Salvadó Artells, M., de Bruin, P.W., et al., 2009. Computed tomography dose assessment for a 160 mm wide, 320 detector row, cone beam CT scanner. *Phys. Med. Biol.* 54, 3141–3159.
- Hein, F., Meyer, T., Hadamitzky, M., et al., 2009. Prospective ECG-triggered sequential scan protocol for coronary dual-source CT angiography: initial experience. *Int. J. Cardiovasc. Imaging* 25, 231–239.
- Herzog, C., Nguyen, S.A., Savino, G., et al., 2007. Does two-segment image reconstruction at 64-section ct coronary angiography improve image quality and diagnostic accuracy. *Radiology* 244, 121–129.
- Huda, W., Tipnis, S., Sterzik, A., et al., 2010. Computed effective dose in cardiac CT. *Phys. Med. Biol.* 55, 3675–3684.
- International Commission on Radiological Protection (ICRP), 2007. Publication 103: the 2007 recommendations of the ICRP. *Ann. ICRP* 37, 62–68.
- Leschka, S., Alkadhi, H., Stolzmann, P., et al., 2008. Mono- versus bisegment reconstruction algorithms for dual source computed tomography coronary angiography. *Invest. Radiol.* 43, 703–711.
- Lin, P.J., Herrnsdorf, L., 2010. Pseudohelical scan for the dose profile measurements of 160 mm wide cone-beam MDCT. *AJR Am. J. Roentgenol.* 194, 897–902.
- Mori, S., Endo, M., Nishizawa, K., et al., 2005. Enlarged longitudinal dose profiles in cone-beam CT and the need for modified dosimetry. *Med. Phys.* 32, 1061–1069.
- Pasricha, S.S., Nandurkar, D., Seneviratne, S.K., et al., 2009. Image quality of coronary 320-MDCT in patients with atrial fibrillation: initial experience. *AJR Am. J. Roentgenol.* 193, 1514–1521.
- van der Bijl, N., de Bruin, P.W., Geleijns, J., et al., 2010. Assessment of coronary artery calcium by using volumetric 320-row multi-detector computed tomography: comparison of 0.5 mm with 3.0 mm slice reconstruction. *Int. J. Cardiovasc. Imaging* 26, 473–482.
- Wu, T.H., Huang, Y.H., Lee, J.J., et al., 2004. Radiation exposure during transmission measurements: comparison between CT- and germanium-based techniques with a current PET scanner. *Eur. J. Nucl. Med. Mol. Imaging* 31, 38–43.